

676420

Anyox

103P 021

Geochemistry and Tectonic Setting of Basalts from the Anyox *Mining*
^{Comp}~~Volcanogenic Massive Sulphide Deposits~~, British Columbia

Alan D. Smith

Department of Earth Sciences,
National Cheng Kung University,
Tainan, Taiwan, ROC

For Canadian Journal of Earth Sciences

26 February 1992

1

look at Dan's
info
Sharpe's thesis

Alan D. Smith, Geochemistry and tectonic setting of basalts from the Anyox volcanogenic massive sulphide deposits, British Columbia.

ABSTRACT

Volcanogenic massive sulphide deposits at Anyox in the Tracy Arm terrane of the Canadian Cordillera are associated with a sequence of tholeiitic basalts with minor intercalated basaltic andesite tuffs and siliceous sediments. Sm-Nd and Pb-Pb systematics indicate a Late Triassic to Middle Jurassic age. The tholeiites are characterised by N-MORB to weak IAT trace element signatures with slight LILE enrichment and HFSE depletion, high $^{207}\text{Pb}/^{204}\text{Pb}$, and $\epsilon\text{Nd}(170\text{Ma})$ values of +8.2 to 8.4. [The mineralised sequence is conformably overlain by argillaceous sediments and minor limestones.] These features, combined with the location of the strata and similarities with the Spider Peak Formation of the Methow terrane, indicate an origin in a narrowing marginal basin which once separated superterrane I and II.

INTRODUCTION

The volcanogenic massive sulphide deposits at Anyox (55°N, 129° 50'W; Fig. 1) ^{produced} at 24.7 million tons ^{grams} 1.6% ^{copper} Cu constitute one of the most important concentrations of mineralisation in the Canadian Cordillera. The sulphide deposits are associated with a sequence of tholeiitic metabasalts and argillaceous sediments (Sharp 1980) and show stratigraphic features intermediate between those of Besshi- and Cyprus-type deposits. The Anyox deposits are located in the Tracy Arm terrane close to the suture between superterrane I (Quesnel, Cache Creek, and Stikine terranes) and II (Wrangell and Alexander terranes) (Fig. 1). The Tracy Arm terrane is a structurally complex, ^{largely} metamorphic terrane which includes elements of both the Alexander terrane to the west and the Stikine terrane to the east (Monger and Berg, 1987; Coney 1989). The formation of the Tracy Arm terrane is related to the accretion of superterrane II to the continental margin, formed by superterrane I, during the mid Cretaceous. The zone of imbrication of the superterrane is marked by west-vergent thrust sheets along the eastern margin of the Alexander terrane (Rubin et al. 1990) but the tectonics of the accretion event are controversial because of differing structural relationships between the Stikine and Alexander terrane throughout the Cordillera. In the central Cordillera at the latitude of Anyox, the Alexander terrane is often considered to unconformably overlie the strata of the Stikine terrane (eg. Crawford et al. 1987). However, in the southern Cordillera, superterrane I and II are separated by terranes (Methow, Tyaughton, Bridge River,

Work done ✓

Hozameen) of the Methow-Tyughton Trough (Fig. 1). The latter terranes have been interpreted as remnants of a marginal basin consumed by the accretion of superterrane II to the continental margin (Ray 1986, Thorkelson and Smith 1989) or to be part of the Cache Creek terrane which was disrupted and translated along the continental margin (Rusmore and Woodsworth 1991). The latter model implies that superterrane I and II were only separated by a single ocean basin, now represented by the Cache Creek terrane, in the Mesozoic and requires some subsequent event such as northward displacement of the Stikine terrane (Wernicke and Klepacki 1988) to account for the present structural relationships of the terranes. The former model implies the existence of two distinct ocean basins in the Mesozoic and does not necessarily require any post-accretion re-arrangement of the terranes. From their location east of the west-vergent thrust system close to the superterrane I-II suture, the tectonic setting of the Anyox deposits provides important constraints on the tectonic evolution of the Cordillera, ~~[in addition to the origin of ore deposits transitional between the Besshi and Cyprus types.]~~

The strata at Anyox are preserved as a roof pendant to the Coast Plutonic Complex on the west side of Observatory Inlet such that their structural relationship to other units of the Tracy Arm terrane are not known (Fig. 2). Sharp (1980) correlated the sequence at Anyox with the upper part of the Karmutsen Formation of the Wrangell terrane on the Queen Charlotte Islands on the basis of similarities between the overlying sedimentary

assemblages. Such correlations are consistent with a single ocean basin model. However, isotopic and geochemical data for the volcanics associated with mineralisation at Anyox presented in this study preclude correlation with the Karmutsen-Nikolai Formation. An origin for the Anyox deposits in an Early to Middle Jurassic marginal basin which once separated superterrane I and II is preferred.

GEOLOGY OF THE ANYOX DISTRICT

The geology of the Anyox district has been described in detail by Sharp (1980). The mineralised succession consists of 600m of pillowed metabasalts with subordinate, localised layers and lenses of basaltic tuff and agglomerate up to 30m thick. Thin, 1cm to several metre-thick meta-chert and carbonaceous phyllite bands occur throughout the basalt sequence (Fig. 3a). Over 500m of metasediments including siltstones, slate, and phyllite conformably overly the basalts and pass upwards into coarse sandstone turbidites. Rare, limestone lenses less than 30cm thick occur in the lower part of the sedimentary succession. Neither the top nor the base of the sequence is preserved.

Mineralisation includes five Cu-Zn deposits, Hidden Creek, Double Ed, Bonanza, Redwing, Eden, and two Cu deposits, Outsider and Eagle (Figs. 2, 3a). The Hidden Creek and Outsider deposits are located at the basalt-sediment contact (Fig. 3b) and may be considered to be of the Besshi-type as defined by Sawkins (1976) or Fox (1984). The other deposits are located within the basalt pile and are associated with only minor chert and carbonaceous

*folding
- faulting
- beds
? strike
+ dip*

*centimetre
↖*

*Other
deposits*

*References to
Dani*

phyllite bands (Fig. 3c). The sedimentary sequence associated with these is more typical of Cyprus-type deposits, though the ophiolite stratigraphy generally included in the definition of Cyprus-type deposits (Sawkins 1976) is lacking. All deposits have undergone some degree of folding, overturning, or localised faulting.

The Hidden Creek deposit is the largest, containing 32 times more Cu than any of the other deposits. In the volcanic pile the mineralisation forms weak disseminated zones around several strongly mineralised stockworks which in turn extend up into massive sulphide lenses enclosed in up to 75m of meta-chert (Fig. 3b). In the upper stratigraphic layers, mineralisation is associated with carbonaceous phyllite and argillite. The main Cu-bearing phase is chalcopyrite, which occurs in the massive layers, while pyrrhotite, pyrite and sphalerite form thin discontinuous layers and lenses. Late quartz veins cutting the argillaceous metasediments also host galena mineralisation, though this phase is absent from the massive sulphide bodies.

The lithological features of the ore deposits suggest formation during breaks in volcanism. Mineralisation processes were stopped either by the resumption of volcanism (Double Ed deposit), or the sealing off of the hydrothermal systems by pyroclastic activity as at the Bonanza deposit or with clastic sediments in the Hidden Creek deposit.

SAMPLING AND ANALYTICAL PROCEDURES

Sampling was directed away from the ore deposits due to

extensive hydrothermal alteration of the basalts at these localities. Four localities representing the mineralised part of the basalt sequence were sampled: JF22 and JF25 taken from west of the Redwing deposit are the oldest samples stratigraphically (Fig. 3a). Samples JF2 to JF19 were taken from the vicinity of the Dam Lakes and represent the volcanism prior to the formation of the Hidden Creek deposit. Sulphide samples were also taken from the Hidden Creek deposit and represent the principal economic mineralisation (pyrite-pyrrhotite-chalcopyrite sample A12, chalcopyrite A2), gangue minerals (pyrrhotite A4 and pyrite A5), and late stage veining (galena A9).

Sample preparation involved sawing of basalt samples into 2mm thick pieces in order to facilitate removal of alteration surfaces and quartz microveins. Saw marks were removed by sanding with silicon-carbide paper, and the samples were then crushed using a tungsten-carbide mill. Major and trace elements V, Ni, Zr, Y, Sr, and Ba were determined by X-ray fluorescence spectroscopy. Instrumental neutron activation analysis was used to determine Cr, Sc, Co, Hf, Ta, U, Th, and all rare earth elements except Sm and Nd which along with Pb were determined by mass spectrometry isotope dilution. Two sigma errors are less than $\pm 20\%$ for Gd, Tb, Ho, Tm, less than $\pm 10\%$ for Ta, U, Yb, Lu, V, Zr, Y, Sr, Ba, $\pm 5\%$ for Th, Hf, La, Ce, Eu, and $\pm 1\%$ for Cr, Sc, Co, Sm, Nd, and Pb.

Isotopic analyses were performed at the University of Alberta using VG354 and Micromass MM30 mass spectrometers for Nd and Pb,

distances
to
deposits?
stratigraphic
pos.
stratigraphic
using
Shaw's
stratigraphy

surface weathering?

respectively. Nd was isolated following the PIGS technique of Smith et al. (1990). Nd isotopic results have been normalised to $^{146}\text{Nd}/^{144}\text{Nd}=0.7219$ and are reported relative to $^{143}\text{Nd}/^{144}\text{Nd}=0.511860$ for the La Jolla standard. Pb was isolated by HBr-HCl anion exchange following decomposition in 25M HF/16M HNO₃ (basalt samples) or 16M HNO₃ (sulphide samples). To extend the range of Pb isotopic composition for geochronological purposes, samples JF9 and JF17 were leached with 2.3M HCl for 1 hour at 80°C. Leachates and residues (L and R, respectively: Table 2) were then analysed for Pb isotopic composition as for the whole rock samples. Pb isotopic ratios were determined using a single Re filament with silica gel-phosphoric acid loading technique. Pb fractionation was monitored using the SRM981 standard, five replicate analyses of which gave mean and two sigma standard deviation values of $^{206}\text{Pb}/^{204}\text{Pb}=16.930\pm 0.008$, $^{207}\text{Pb}/^{204}\text{Pb}=15.486\pm 0.010$, $^{208}\text{Pb}/^{204}\text{Pb}=36.696\pm 0.040$ compared to certified values of 16.936, 15.491, 36.721 for this standard.

BASALT GEOCHEMISTRY

The strata at Anyox have been metamorphosed to greenschist grade such that the mineralogy of the basalts consists of actinolite, chlorite, sericite, calcite and albite. The most significant alteration effects reported by Sharp (1980) on basalts proximal to the orebodies involved loss of Ca and Al, and increase of Fe, Mg and Ti, largely as a result of the breakdown of plagioclase. Gain of Si, Na, and dilution of Fe, Mg was also noted accompanying albitisation. None of these effects are evident in the samples in Table 1, which with the exception

now

?

of JF2, are similar to N-MORB in major element composition. Loss on ignition values of 0.72 to 2.1 weight percent are considered low for greenschist facies basalts and attest to only minor alteration and the precautions taken in sample preparation. Nonetheless, conclusions regarding the petrogenetic setting of the volcanics are based largely on the minor and trace elements which are considered immobile under such metamorphic conditions. The list of such includes the rare earth elements (REE), high field strength elements (HFSE: Ti, Zr, Hf, Nb, Ta, P, V) and the large ion lithophile element (LILE) Th.

— see other
— ? data
all ?

Distinct variations are noted between trace element chemistry and stratigraphic position: samples early in the volcanic pile (JF22 and JF25) are tholeiites with trace element abundances similar to N-MORB (Fig. 4a). Subsequent samples, JF3 and JF9, are more refractory, and are characterised by low TiO₂ (1.17 wt. %) and low trace element abundances relative to N-MORB, although their trace element profiles are predominantly flat. Peaks at Ta in the trace element profile may be an artifact of the high uncertainty in the measurement of low abundances of this element, combined with depiction on a log scale. Samples JF10 to JF15 have more evolved compositions whose low Ni, Cr, MgO and Eu*/Eu, but similar LILE, REE, and HFSE abundances to N-MORB are likely the result of differentiation. The volcanism prior to formation of the Hidden Creek deposit (JF17 to JF 19) is characterised by by a weak island arc tholeiite (IAT) signature of low FeO*/MgO ratios (1.1 to 1.2) and enrichment in LILE and HFSE relative to N-MORB which imparts a distinct slope to the trace element profile (Fig.

4a). Ni and Cr abundances are low in these samples despite moderately high MgO contents.

Sample JF2 with 55% SiO₂ is a basaltic andesite tuff with a distinct calc-alkaline signature including low FeO*/MgO (1.0), and low HFSE content (eg. 0.96 wt % TiO₂, 0.09 ppm Ta). A similar proportion of comparable compositions was noted in the volcanic pile prior to the formation of the Hidden Creek deposit by Sharp (1980). This would suggest that the tuffs are distributed throughout the section and comprise approximately 5 percent of the volcanism.

ISOTOPIC COMPOSITION

Dating of the samples is limited in resolution by the small variation in isotopic composition (Table 2). The Pb isotopic composition of sulphides A4, A9, and A2 define an isochron of 168±37 Ma (Fig. 5). Most basalt samples, including the results of the leaching experiments, can be fit by a line of similar to slightly greater slope corresponding to ages between 170 and 260 Ma (Fig. 5). Similarly, with the exception of JF2 and JF19 which have distinct Pb isotopic compositions, the basalt samples show a positive correlation of ¹⁴⁷Sm/¹⁴⁴Nd and ¹⁴³Nd/¹⁴⁴Nd which corresponds to an age of approximately 194Ma (Fig. 6).

Uncertainties in the age of the Anyox sequence do not affect the interpretation of the isotopic ratios. Correction of the ¹⁴³Nd/¹⁴⁴Nd ratios for Late Triassic to Middle Jurassic ages yields εNd(T) values between +8.0 and +8.6, within the range for

early Mesozoic N-MORB and primitive arcs (Fig. 7). The lowest ϵ_{Nd} value of +7.8 is shown by JF2, otherwise there is no significant correlation with stratigraphic position.

The Pb contents of the basalts at 1.1 to 2.2 ppm are higher than for N-MORB, which average about 0.4 ppm (eg. Vidal and Clauer 1981). As a result, the Anyox basalts have low k (7.6 to 26.5) and μ values (3.2 to 8.4) relative to N-MORB (typically $k=32$, $\mu=8.2$, eg. Sun 1980). Using the measured μ and k values results in minor age corrections of up to 0.30, 0.02, and 0.35 for $^{206}\text{Pb}/^{204}\text{Pb}$, $^{207}\text{Pb}/^{204}\text{Pb}$, and $^{208}\text{Pb}/^{204}\text{Pb}$, respectively (Table 2). Even on doubling of the age correction by assuming N-MORB-like μ and k values, the corrected ratios would still be characterised by high $^{207}\text{Pb}/^{204}\text{Pb}$ and $^{208}\text{Pb}/^{204}\text{Pb}$ relative to the field for early Mesozoic N-MORB (Fig. 5). The Pb isotopic compositions of the basalts are also independent of stratigraphic position, though the parallel trends in $^{207}\text{Pb}/^{204}\text{Pb}$ - $^{206}\text{Pb}/^{204}\text{Pb}$ space indicate differing initial ratios between the basalts and the sulphide minerals from the higher stratigraphic levels. The higher $^{207}\text{Pb}/^{204}\text{Pb}$ ratios of the sulphides could be accounted for by the incorporation of Pb from the surrounding sediments as the hydrothermal system forming the ore deposits was sealed by increasing sediment input, or by exchange of Pb with local tuffitic compositions such as JF2. The similar isotopic composition of galena sample A9 to sulphides of the Hidden Creek deposit suggests an origin on remobilisation of Pb from the main ore bodies.

The overall low trace element abundances, presence of weak IAT signatures, high $^{207}\text{Pb}/^{204}\text{Pb}$ ratios, and high $\epsilon\text{Nd}(170\text{ Ma})$ values of the Anyox basalts are characteristic of a back-arc or marginal basin setting. The progression from siliceous to argillaceous sedimentation favours the latter. In such environments, LILE enrichment and high $^{207}\text{Pb}/^{204}\text{Pb}$ ratios may be imparted by contamination of a N-MORB source with material from a nearby arc-source or by young subcontinental lithosphere. The latter commonly has an arc source component inherited from subduction processes along the continental margin. Both the Alexander and Stikine terranes contain earlier volcanic arc assemblages, such that an origin proximal to either terrane is consistent with the geochemistry of the volcanics at Anyox.

A marginal basin origin also accounts for the transitional nature of the mineralisation between Besshi- and Cyprus type deposits. As pointed out by Smith (1991), the stratigraphy of ore deposits is not necessarily diagnostic of tectonic setting. The presence of argillaceous sediments or ophiolite stratigraphy classically used to define such deposits (eg. Sawkins 1976, Fox 1984) will depend on the sediment input into the basin and the amount of disruption on accretion.

COMPARISON WITH THE KARMUTSEN-NIKOLAI FORMATION

The Karmutsen Formation of the Wrangell terrane in British Columbia, and its equivalents, the Nikolai Formation in Alaska and the Chilcat basalt of the Taku terrane (Fig. 1), comprise a

3000 to over 6000 metre-thick late Middle Triassic to early Late Triassic tholeiite-ferrotholeiite sequence (Davis and Plafker 1985, Barker et al. 1989) (Table 3). Tholeiites, characterised by high MgO contents (9.4 to 10.3 wt. %) and flat N-MORB normalised trace element patterns with minor Th enrichment (Fig. 4b) are found on the Queen Charlotte Islands. However, ferrotholeiites, characterised by more evolved compositions (eg. MgO contents of less than 7 wt. %) and mixed ocean island basalt (OIB) -IAT trace element signatures of coupled HFSE and LILE enrichment (Fig. 4c), comprise much of the Formation. The latter signature was imparted to the Karmutsen by contamination of MORB with the remnant island arc source of the Sicher Group (Barker et al. 1989). Although several Anyox basalts such as JF3 to JF9 resemble the Karmutsen-Nikolai tholeiites, equivalents of the ferrotholeiite type are not found at Anyox. Minor HFSE and LILE enrichments are seen in the later Anyox basalts such as JF17 to JF19, but the signature is not as developed as in the Karmutsen-Nikolai Formation.

$\epsilon_{\text{Nd}}(220\text{Ma})$ values of the Karmutsen Formation from the Wrangell terrane range from +6.2 to +7.3 (Fig. 7) (Samson et al. 1990). This range is extended to +5.5 to +7.8 with the inclusion of data for the Tats basalts at the Windy Craggy ore deposit in the Alexander terrane (Smith and Fox 1989) which are probable equivalents of the Karmutsen-Nikolai Formation. The $\epsilon_{\text{Nd}}(220\text{Ma})$ values of the Karmutsen-Nikolai Formation are thus significantly lower than for the Anyox volcanics. The Anyox volcanics also tend to have higher $^{206}\text{Pb}/^{204}\text{Pb}$ ratios (Fig. 5).

Significant differences also exist in the nature of the overlying sedimentary succession: the Karmutsen-Nikolai Formation is overlain by up to 300 metres of limestone (the Quatsino Formation on Vancouver Island, the Kunga Formation on the Queen Charlotte Islands, and the Chichistone limestone in the Wrangell Mountains; Jones et al. 1977, Davis and Plafker 1985) which include only subordinate argillaceous sediments, and are indicative of an open ocean environment. In contrast, at Anyox, limestones (Swamp Point member, Sharp 1980) are subordinate to argillaceous sediments, more typical of a marginal basin environment. These lithological and geochemical differences are considered sufficient to preclude affiliation with the Karmutsen-Nikolai Formation.

CORRELATION WITH VOLCANIC TERRANES IN THE METHOW-TYAUGHTON TROUGH

The Methow-Tyaughton Trough contains late Paleozoic and Mesozoic oceanic terranes separated from superterrane I and II by the Fraser and Pasayten Fault systems. In the western part of the Trough, the Bridge River and Hozameen terranes comprise Late Permian to Middle Jurassic chert, argillite, basalt, and minor carbonates (Monger 1985, Monger and Berg 1987). The principal volcanic assemblages of these terranes ^{are} ~~is~~ the Late Permian to Middle Jurassic Hozameen Group of the Hozameen terrane and equivalents in the Bridge River terrane. The Hozameen Group includes basalts with IAT signatures and basaltic andesites at the base of the volcanic sequence, with a weak OIB signatures becoming prevalent toward the top of the Group (Ray 1986). These features have been interpreted to indicate a back-arc basin

environment in which there later developed ocean island volcanism (Ray 1986). Both IAT and OIB types show significant compositional differences with the Anyox volcanics (Table 3).

Along the eastern margin of the Trough, the Methow and Tyaughton terranes comprise Middle Triassic to Early Cretaceous volcanics and clastic sedimentary rocks with minor limestones (Monger and Berg 1987). The principal volcanic assemblage is the Middle Triassic Spider Peak Formation of the Methow terrane, which comprises up to 500 metres of massive to pillowed metabasalts with locally important tuff and chert horizons toward the top of the volcanic pile (Ray 1986). The Formation is overlain unconformably by Late Jurassic argillaceous sediments of the Ladner Group (Ray 1986, O'Brien 1987). In the lower part of the Formation, tholeiites have high Na and low Ca contents indicating significant albitisation. SiO₂ and TiO₂ contents are also high relative to N-MORB but as these elements usually behave in an opposite manner during albitisation, the combination may indicate slightly more evolved basalt compositions such as found at Anyox. Trace element profiles (Fig. 4d) are characterised by low Ni, Cr but HFSE abundances up to 1.3 times N-MORB, similar to JF10 to JF15. Basalts with weak IAT signatures including low HFSE contents become more important toward the top of the Formation, though these show significant alteration which could exaggerate their resemblance to IAT and it is not possible to determine whether this type might be an equivalent of Anyox basalts such as JF3 and JF9. The principle difference between the Anyox sequence and Spider Peak Formation is the presence of gabbros in the lower

part of the Spider Peak Formation which suggest a possible ophiolite stratigraphy. However, as the base of the Anyox sequence is not preserved, the lack of gabbros is not diagnostic. Considering the uncertainties in the age of the Anyox sequence, and that the timing of the termination of volcanism in the Spider Peak Formation is unknown, the geochemical resemblance of the two volcanic sequences suggests at least a similar tectonic origin.

TECTONIC MODEL

The Anyox sequence and Spider Peak Formation indicate that remnants of a Middle Triassic to Middle Jurassic marginal basin can be traced along the suture of superterrane I and II for much of the length of the Cordillera. The age and regional extent of this basin conflicts with interpretations (eg. Rusmore and Wordsworth 1991) that the Methow-Tyughton Trough terranes are localised fragments of the Cache Creek terrane displaced along the margin of superterrane I. The preferred tectonic model is thus that of Thorkelson and Smith (1989) where accretion of superterrane II takes place by the subduction of a marginal basin beneath the western margin of superterrane I. The tectonic setting of the Anyox volcanics and Spider Peak Formation relative to the evolution of this basin is illustrated in Fig. 8: In the Late Permian and Early Triassic the Stikine and Quesnel terranes were separated by the Cache Creek ocean, while the Stikine and Wrangell-Alexander terranes were separated by a second basin, remnants of which are now found at Anyox and in the Methow

terrane (Fig. 8a). The Quesnel, Cache Creek, and Stikine terranes amalgamated in the Late Triassic by the subduction of the Cache Creek terrane beneath Quesnellia (eg. Coney 1989), generating the calc-alkaline volcanics of the Nicola Group (Fig. 8b). Meanwhile, an ocean ridge system in the second basin interacted with the margin of the Stikine or Quesnel terrane to produce the upper part of the Spider Peak Formation.

The amalgamation of superterrane I and its subsequent accretion to North America in the Early Jurassic resulted in uplift which provided the Methow-Tyaughton basin with a sediment source to the east. The resulting influx of argillaceous sediments sealed off ore forming hydrothermal systems such as at the Hidden Creek deposit (Fig. 8c). The initial contraction of the Methow-Tyaughton basin is marked by the obduction of the Hozameen and Bridge River terranes onto the eastern margin of superterrane II in the Middle Jurassic (Fig. 8c) (Thorkelson and Smith 1989). Interpretations that the Hozameen and Bridge River terranes were accreted to superterrane I at this time (Rusmore et al. 1988) conflict with the record of sedimentation in the Methow and Tyaughton terranes. Subduction of the basin resulted in generation of calc-alkaline volcanics of the Spences Bridge Group along the western margin of superterrane I (Fig. 8d). Models which invoke only a single ocean basin cannot account for the presence of this arc. After the Middle Jurassic, sediment sources to the west of the Methow and Tyaughton terranes interdigitate with sources to the east marking the final stages of basin contraction (Thorkelson and Smith 1989). Closure of the basin

occurred in the mid Cretaceous as marked by a change from calc-alkaline to calc-alkaline-intraplate signatures in the Spences Bridge Group (Thorkelson and Smith 1989). Obduction of the Anyox sequence and Spider Peak Formation probably took place during these final stages of basin contraction (Fig. 8d).

The model presented does not necessarily conflict with correlations of the Cache Creek, Bridge River, and Hozameen terranes. These terranes may represent remnants of the eastern ocean basin, disrupted by the translation of the Stikine terrane along the continental margin as depicted by Wernicke and Klepacki (1988). However, an origin for the Bridge River and Hozameen terranes as part of the western ocean basin is more consistent with evidence for their obduction onto the eastern margin of superterrane II prior to closure of the Methow-Tyughton Trough. This event also implies an origin proximal to superterrane II, where the change from marginal basin (weak IAT) to weak rift (OIB) signatures might be accounted for by progressive interaction with the source of the Karmutsen-Nikolai Formation (Fig. 8b).

CONCLUSIONS

The association of the Anyox volcanogenic massive sulphide deposits with tholeiites and calc-alkaline tuffs, in conjunction with a transition from siliceous to argillaceous sedimentation, suggests formation in a narrowing marginal basin. Geochemical and isotopic features of the Anyox volcanics are different from contemporaneous assemblages in the Wrangell and Alexander

terrane, but may be tentatively correlated with a marginal basin assemblage in the Methow terrane. Tectonic elements of a second ocean basin in addition to possible Cache Creek terrane correlatives are thus present in the western Cordillera, supporting tectonic models whereby accretion of superterrane II occurred by eastward-directed subduction beneath the western margin of superterrane I in the mid Cretaceous.

ACKNOWLEDGEMENTS

G. Kennedy and J. St.Pierre are thanked for assistance with the irradiation of samples at the École Polytechnique SLOWPOKE facility. XRF analyses were performed at McGill University by T. Amhedali. J.N. Ludden is thanked for comments on an earlier version of the manuscript.

REFERENCES

- ANDREW, A., and GODWIN, C.I. 1989. Lead and strontium-isotope geochemistry of the Karmutsen Formation, Vancouver Island, British Columbia. *Canadian Journal of Earth Sciences*, 26:908-919.
- BARKER, F., SUTHERLAND-BROWN, A., BUDAHA, J.R., and PLAFKER, G. 1989. Back-arc with frontal-arc component origin of Triassic Karmutsen basalt, British Columbia. *Chemical Geology*, 75:81-102.
- CHURCH, S.E. 1976. The Cascade Mountains revisited: a re-evaluation in light of new lead isotopic data. *Earth and Planetary Science Letters*, 29:175-188.
- CONEY, P.J. 1989. structural aspects of suspect terranes and accretionary tectonics in western North America. *Journal of Structural Geology*, 11:102-125.
- CRAWFORD, M.L., HOLLISTER, L.S., and WOODSWORTH, G.J. 1987. Crustal deformation and regional metamorphism across a terrane boundary, Coast Plutonic Complex, British Columbia. *Tectonics*, 6:343-361.
- DAVIS, A., and PLAFKER, G. 1985. Comparative geochemistry and petrology of Triassic basaltic rocks from the Taku terrane on the Chilcat Peninsula and Wrangellia. *Canadian Journal of Earth Sciences*, 22:183-194.
- FOX, J.S. 1984. Besshi-type volcanogenic sulphide deposits- a

review. Canadian Institute of Mining and Metallurgy Bulletin, April 1984, pp. 57-76.

JONES, D.L., SILBERLING, N.J. and HILLHOUSE, J. 1977. Wrangellia - A displaced terrane in northwestern North America. Canadian Journal of Earth Sciences, 14:2565-2577.

MONGER, J.W.H. 1985. Structural evolution of the southwestern Intermontane belt, Ashcroft and Hope map areas, British Columbia. In Current Research Part A, Geological Survey of Canada Paper 85-1A, pp. 349-358.

MONGER, J.W.H., and BERG, H.C. 1987. Lithotectonic terrane map of western Canada and southeastern Alaska. United States Geological Survey Map 1874B, 12p.

O'BRIEN, J.A. 1987. Jurassic biostratigraphy and evolution of the Methow-Trough, southwestern British Columbia. M.Sc. thesis, University of Arizona, Tucson.

RAY, G.E. 1986. The Hozameen fault system and related Coquihalla serpentine belt of southwestern British Columbia. Canadian Journal of Earth Sciences, 23:1022-1041.

RUBIN, C.M., SALEEBY, J.B., COWAN, D.S., BRANDON, M.T. and MCGRODER, M.F. 1990. Regionally extensive mid-Cretaceous west-vergent thrust system in the northwestern Cordillera: Implications for continent margin tectonism. Geology, 18:276-280.

RUSMORE, M.E. and WOODSWORTH, G.J. 1991. Distribution and

tectonic significance of Upper Triassic terranes in the eastern Coast Mountains and adjacent Intermontane Belt, British Columbia. *Canadian Journal of Earth Sciences*, 28:532-541.

RUSMORE, M.E., POTTER, C.J., and UMHOEFER, P.J. 1988. Middle Jurassic terrane accretion along the western edge of the Intermontane superterrane, southwestern British Columbia. *Geology* 16, 891-894.

SAMSON, S.D., PATCHETT, P.J., GEHRELS, G.E., and ANDERSON, R.G. 1990. Nd and Sr isotopic characterisation of the Wrangellia terrane and implications for crustal growth of the Canadian Cordillera. *Journal of Geology*, 98:749-762.

SAUNDERS, A.D., and TARNEY, J. 1984. Geochemical characteristics of basaltic volcanism within back-arc basins. In *Marginal basin geology*. Edited by B.P. Kokelaar and M.F. Howells. Blackwell Scientific, pp. 59-76.

SAWKINS, F.J. 1976. Massive sulphide deposits in relation to geotectonics. In *Metallogeny and plate tectonics*. Edited by D.F. Strong. Geological Association of Canada Special Paper 14, pp. 221-240.

SHARP, R.J. 1980. The geology, geochemistry and sulphur isotopes of the Anyox massive sulphide deposits. M.Sc. thesis, University of Alberta, Edmonton.

SILBERLING, N.J., JONES, D.L., BLAKE, M.C., and HOWELL, D.G. 1987. Lithotectonic terrane map of the western conterminous United States. United States Geological Survey Map 1874C, 20p.

- SMITH, A.D. 1991. Reply to the comment by A.P. Boyle and R.K. Westhead. *Mineralium Deposita* 26:242-244.
- SMITH, A.D. 1986. Isotopic studies of Terrane I, south-central British Columbia. Ph.D. thesis, University of Alberta, Edmonton.
- SMITH, A.D. and FOX, J.S. 1989. Geochemistry of basalts from the Windy Craggy and Anyox volcanogenic massive sulphide deposits, British Columbia. GAC-MAC Program with Abstracts, 14:A22.
- SMITH, A.D., GILLIS, K.M., and LUDDEN, J.N. 1990. A Pre-Irradiation Group Separation (PIGS) technique for the analysis of rare-earth elements during Nd isotopic analysis of geological samples. *Chemical Geology*, 81:17-22.
- SMITH, A.D., FOX, J.S., FARQUHAR, R.M., and SMITH, P.E. 1990. Geochemistry of Ordovician Koli Group basalts associated with Besshi-type Cu-Zn deposits from the southern Trondheim and Sulitjelma mining districts of Norway. *Mineralium Deposita*, 25:15-24.
- SUN, S.-S. 1980. lead isotopic study of young volcanic rocks from mid-ocean ridges, ocean islands and island arcs. *Philosophical Transactions of the Royal Society of London, Series A*, 297:409-445.
- THORKELSON, D.J., and SMITH, A.D. 1989. Arc and intraplate volcanism in the Spences Bridge Group: Implications for Cretaceous tectonics in the Canadian Cordillera. *Geology*,

VIDAL, Ph., and CLAUER, N. 1981. Pb and Sr isotopic systematics of some basalts and sulphides from the East Pacific Rise at 21° N (project RITA). *Earth and Planetary Science Letters*, 55:237-246.

WERNICKE, B. and KLEPACKI, D.W. 1988. Escape hypothesis for the Stikine block. *Geology*, 16:461-464.

WHITE, W.M., and PATCHETT, J. 1984. Hf-Nd-Sr isotopes and incompatible element abundances in island arcs: Implications for magma origins and crust mantle evolution. *Earth and Planetary Science Letters* 67:167-185.

FIGURE CAPTIONS

1. Location of the Anyox deposits in relation to the accreted terranes of the Canadian Cordillera. (after Monger and Berg 1987, Silberling et al. 1987). *more recent references*
2. Geology of the Anyox district showing the distribution of ore deposits and sampling localities (after Sharp 1980).
3. (a) Composite stratigraphic column of mineralised strata at Anyox showing the location of ore deposits and basalt samples. (b) stratigraphic column of the Hidden Creek deposit (c) stratigraphic column of the Double Ed deposit (*after* Sharp 1980) *from?*
4. N-MORB normalised trace element variation diagrams for (a) Anyox volcanics; (b, c) Karmutsen-Nikolai Formation (Davis and Plafker 1985, Barker et al. 1989); (d) Spider Peak Formation (Ray 1986). N-MORB values, in ppm (from Saunders and Tarney 1984): Th 0.2, Ta 0.17, Ce 10, P 570, Zr 88, Hf 2.5, Sm 0.33, Ti 8400, Y 35, Yb 3.5, Ni 138, Cr 290, V 250 (assumed).
5. Pb isotopic composition of Anyox volcanics and sulphides relative to MORB, the Karmutsen-Nikolai Formation (Andrew and Godwin 1989) and oceanic sediments (Church 1976). Age corrections made assuming $\mu=8.2$, $k=23$ for the N-MORB-source.
6. Sm-Nd isochron diagram for the Anyox volcanics.
7. ϵ_{Nd} values for the Anyox volcanics relative to data for late Paleozoic to Recent oceanic assemblages. Evolution curves

denote typical ranges for MORB (solid lines) and primitive arcs (broken lines). In order of increasing age: Ocean ridge assemblages: MM modern MORB; CM Cretaceous MORB; SO Semail ophiolite; KN Karmutsen-Nikolai Formation (Samson et al. 1990); CC Cache Creek Group (Smith, unpublished data); FF Fennell Formation; UO Urals ophiolite; KR Kings River ophiolite; KG Koli Group; BOI Bay of Islands ophiolite (data sources, except where indicated, are given in Smith et al. 1990). Primitive arcs: PA modern primitive arcs (eg. White and Patchett 1984); SB Spences Bridge Group (Thorkelson and Smith 1989); NG Nicola Group (Smith 1986).

8. Tectonic model for the formation of the Anyox volcanogenic massive sulphide deposits relative to the closure of the Methow-Tyaughton Trough. Abbreviations: BR: Bridge River terrane; CC: Cache Creek terrane; HZ: Hozameen terrane; Hz. Gp.: Hozameen Group; M: Methow terrane; QN: Quesnel terrane; SBG: Spences Bridge Group; SP: Spider Peak Formation; ST: Stikine terrane; T: Tyaughton terrane; II: superterrane II.

Table 1. Anyox major and trace element results

	JF2	JF3	JF9	JF10	JF12	JF14	JF15	JF17	JF18	JF19	JF22
SiO2	55.35	48.52	50.26	50.62	48.46	46.44	48.40	50.96	50.27	50.69	50.35
TiO2	0.96	1.17	1.17	1.48	1.38	1.48	1.41	1.50	1.49	1.44	1.38
Al2O3	13.84	16.96	16.89	16.94	15.47	16.72	16.99	15.22	14.60	15.18	14.48
Fe2O3	9.73	11.09	10.94	12.21	12.48	13.78	11.77	11.68	12.32	11.55	12.73
MnO	0.22	0.16	0.23	0.17	0.17	0.20	0.17	0.15	0.15	0.15	0.27
MgO	8.43	8.14	7.18	7.66	8.97	8.82	6.17	8.84	9.39	9.30	9.17
CaO	7.55	11.31	9.74	6.98	10.57	10.21	10.21	12.95	8.94	8.67	8.14
Na2O	3.72	2.24	3.23	3.71	2.13	2.05	1.83	2.99	2.59	2.77	3.04
K2O	0.10	0.29	0.26	0.09	0.24	0.15	0.17	0.14	0.10	0.11	0.32
P2O5	0.09	0.10	0.09	0.14	0.12	0.15	0.14	0.15	0.14	0.16	0.11
LOI	1.65	1.55	1.14	2.10	1.87	2.13	0.72	1.47	1.54	1.50	2.07
V	196	250	281	280	261	273	284	322	311	307	303
Cr	245	250	268	188	395	219	199	167	169	157	123
Ni	121	126	89	81	161	94	60	44	56	52	61
Zr	71	81	81	101	95	100	97	104	104	104	88
Y	21	23	24	33	31	30	31	30	29	30	29
Sr	96	151	215	100	101	108	123	204	186	204	106
Ba	83	117	153	96	95	124	70	185	72	129	219
Sc	37	38	43	39	44	39	38	38	45	43	49
Co	43	47	42	39	52	44	41	37	43	39	44
Hf	1.54	1.86	1.88	2.63	2.32	2.38	2.36	2.67	2.49	2.36	2.11
Ta	0.09	0.26	0.27	0.27	0.24	0.26	0.25	0.28	0.33	0.27	0.13
U	--	0.07	0.11	0.07	0.18	--	--	--	--	0.18	0.12
Th	0.20	0.16	0.25	0.18	--	0.24	--	0.59	0.44	0.36	0.28
Pb	1.29	--	2.17	1.13	--	--	--	1.48	--	1.37	--
La	2.43	2.73	2.59	3.63	3.24	2.87	3.28	4.51	4.40	4.46	2.73
Ce	7.17	7.21	7.81	9.75	8.71	8.25	9.42	11.0	11.6	10.5	6.99
Nd	7.86	5.77	7.21	9.55	8.37	8.99	8.55	11.2	10.6	10.0	7.74
Sm	2.86	2.58	2.52	3.60	3.26	3.13	3.35	3.61	3.45	3.09	2.93
Eu	0.67	0.90	0.76	0.88	0.97	0.51	1.10	0.90	0.85	1.14	0.91
Gd	3.40	--	3.32	4.54	4.30	4.03	4.84	4.08	--	3.94	3.64
Tb	0.57	0.58	0.62	0.85	0.79	0.75	0.78	0.86	--	--	0.70
Ho	0.83	0.95	1.06	1.38	1.31	1.19	1.32	1.26	1.39	1.13	1.14
Tm	--	--	--	0.54	0.54	0.50	0.59	--	--	--	--
Yb	2.40	2.68	2.69	3.56	3.42	3.33	3.37	3.21	3.25	3.13	3.19
Lu	0.32	0.42	0.42	0.56	0.52	0.50	0.53	0.51	0.51	0.49	0.49
La/Ybn	0.67	0.67	0.64	0.67	0.63	0.57	0.64	0.93	0.89	0.94	0.57
Eu/Eu*	0.66	0.91	0.83	0.66	0.80	0.45	0.85	0.67	0.63	1.02	0.85

Notes: Major elements have been recalculated to 100 wt% on a volatile free basis, although the original loss on ignition (LOI) has been included as a measure of alteration. Trace element concentrations are in ppm.

prefer original values

Table 2. Isotopic results

	Sm/Nd	$\frac{143\text{Nd}}{144\text{Nd}}$ m	$\frac{143\text{Nd}}{144\text{Nd}}$ c	Nd (170Ma)	μ	k	$\frac{206\text{Pb}}{204\text{Pb}}$ m	$\frac{207\text{Pb}}{204\text{Pb}}$ m	$\frac{208\text{Pb}}{204\text{Pb}}$ m	$\frac{206\text{Pb}}{204\text{Pb}}$ c	$\frac{207\text{Pb}}{204\text{Pb}}$ c	$\frac{208\text{Pb}}{204\text{Pb}}$ c
Basalts												
JF2	0.364	0.513063 ±6	0.512818	+7.8		10.2	19.102 ±.006	15.601 ±.006	38.531 ±.011			38.445
JF9	0.350	0.513072 ±7	0.512836	+8.2	3.2	7.6	19.007 ±.005	15.582 ±.003	38.425 ±.013	18.921	15.578	38.361
JF9-R							18.981 ±.002	15.580 ±.003	38.441 ±.005			
JF10	0.376	0.513099 ±10	0.512846	+8.3	4.0	10.5	19.105 ±.006	15.588 ±.005	38.558 ±.012	18.998	15.583	38.469
JF17	0.323	0.513062 ±9	0.512845	+8.2		26.5	19.020 ±.005	15.577 ±.006	38.493 ±.010			38.262
JF17-L							18.911 ±.010	15.572 ±.008	38.345 ±.013			
JF17-R							19.045 ±.006	15.580 ±.006	38.544 ±.017			
JF19	0.308	0.513056 ±5	0.512849	+8.4	8.4	17.4	18.915 ±.007	15.543 ±.008	38.349 ±.017	18.690	15.533	38.202
JF22	0.379	0.513095 ±5	0.512840	+8.2			18.899 ±.010	15.537 ±.008	38.327 ±.020			
							19.022 ±.004	15.608 ±.003	38.531 ±.008			
Sulphides												
A2 chalcopyrite							19.301 ±.006	15.611 ±.006	38.315 ±.011			
A4 pyrrhotite							18.826 ±.007	15.587 ±.008	38.382 ±.015			
A5 pyrite							18.694 ±.005	15.538 ±.005	38.205 ±.020			
A9 galena							19.048 ±.006	15.599 ±.006	38.505 ±.017			
A12 mixed							19.243 ±.010	15.587 ±.006	38.259 ±.008			

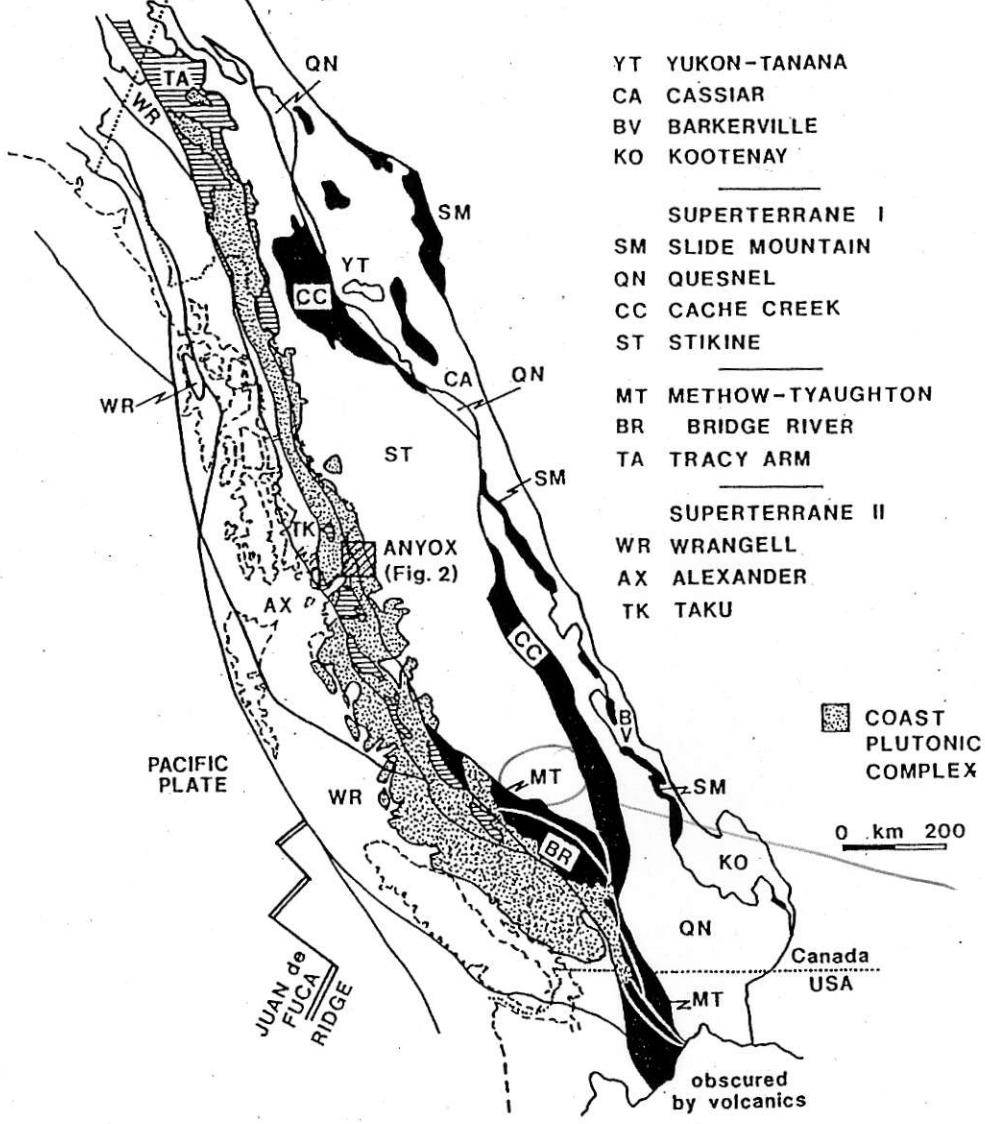
Table 3. Average compositions (with σ_N-1 standard deviations) of Cordilleran oceanic terrane volcanic assemblages

	Anyox n=10	Hozameen Group		Spider Peak Formation n=7	Karmutsen Formation	
		IAT n=9	OIB n=6		tholeiite n=3	ferrotholeiite n=9
SiO ₂	49.50 ±1.46	51.03 ±1.57	50.10 ±0.70	51.00 ±1.14	46.88 ±1.10	49.10 ±0.57
TiO ₂	1.39 ±0.12	0.91 ±0.36	2.59 ±0.81	1.81 ±0.14	1.10 ±0.06	2.00 ±0.32
Al ₂ O ₃	15.94 ±1.05	14.88 ±1.09	15.58 ±0.70	15.19 ±0.85	16.69 ±0.15	14.14 ±0.65
Fe ₂ O ₃	12.05 ±0.84	11.75 ±2.14	12.03 ±1.06	11.82 ±0.95	12.79 ±2.10	13.72 ±1.14
MnO	0.18 ±0.04	0.21 ±0.03	0.21 ±0.05	0.20 ±0.01	0.18 ±0.01	0.22 ±0.06
MgO	8.36 ±1.06	8.04 ±1.59	6.47 ±1.65	7.57 ±0.60	9.68 ±0.44	6.68 ±0.74
CaO	9.77 ±1.69	9.74 ±1.69	8.75 ±1.07	7.30 ±1.67	9.80 ±1.23	11.04 ±1.33
Na ₂ O	2.66 ±0.60	2.94 ±0.61	3.48 ±0.51	4.62 ±0.62	2.52 ±0.34	2.62 ±0.66
K ₂ O	0.19 ±0.08	0.43 ±0.28	0.77 ±0.62	0.35 ±0.33	0.27 ±0.04	0.28 ±0.24
P ₂ O ₅	0.13 ±0.02			0.12 ±0.07	0.10 ±0.01	0.18 ±0.03
Cr	213 ± 77	236 ±133	143 ±111	171 ± 62	406 ± 82	188 ± 84
Ni	82 ± 37				274 ± 84	84 ± 15
Zr	95 ± 9	52 ± 25	148 ± 52	101 ± 13	72 ± 1	122 ± 20
Y	29 ± 3	21 ± 10	19 ± 6	39 ± 5	24 ± 4	27 ± 4
Sc	42 ± 4				37 ± 1	43 ± 4
Co	43 ± 4				62 ± 13	47 ± 3
Hf	2.31±0.28				1.47±0.15	2.73±0.42
Ta	0.26±0.05				0.18±0.10	0.60±0.12
U	0.12±0.05				0.20±0.10	0.28±0.17
Th	0.31±0.14				0.22±0.07	0.78±0.17
La	3.44±0.76				2.70±1.05	8.60±1.67
Sm	3.15±0.38				2.03±0.15	3.92±0.59
Yb	3.18±0.29				2.13±0.57	2.50±0.32
La/Sm	1.1				1.3	4.5
Zr/Y	3.3				3.0	4.5
Th/Hf	0.13				0.15	0.29

All major elements recalculated to 100 weight % on a volatile free basis
Trace elements in ppm

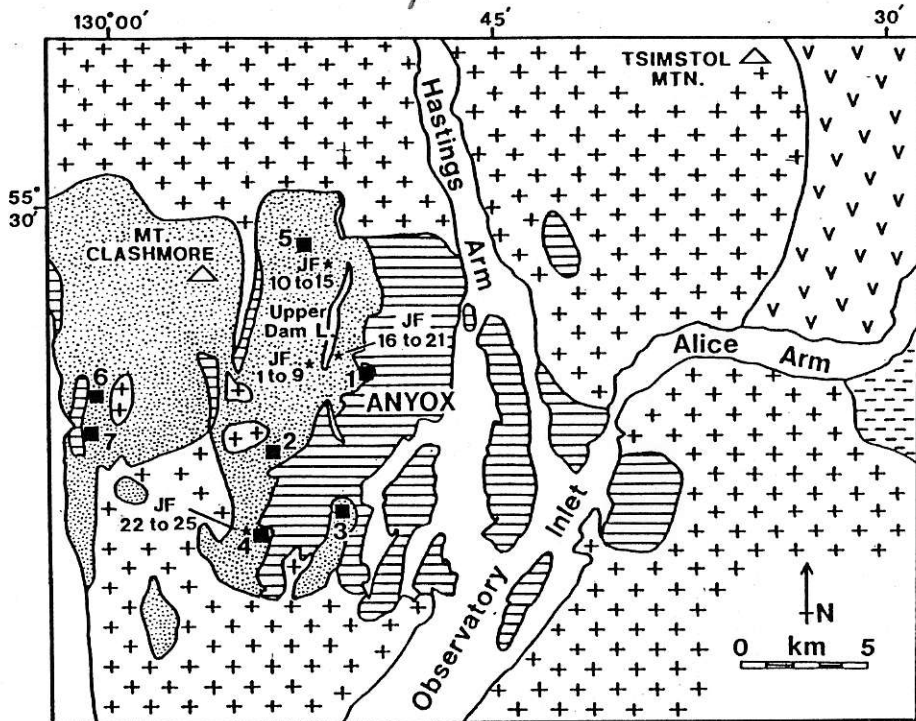
Data sources: Hozameen Group: Ray (1986)
Spider Peak Formation: Ray (1986)
Karmutsen Formation: Barker et al. (1989)

TERRANE MAP OF THE CANADIAN CORDILLERA



not clear highlight?

FIG. 1



⊕ Coast Plutonic Complex

▢ Bowser Lake Group

∇ Hazelton Group

▨ Metasediments

▩ Metabasalt

■ Mineral deposits

1 Hidden Creek

2 Double Ed

3 Bonanza

4 Redwing

5 Eden

6 Outsider

7 Eagle

VMS

- are others in area

- gold

could be altered

Group?

old smelter & town site

FIG. 2

Might consider
Fig 1.A blowup
of terranes

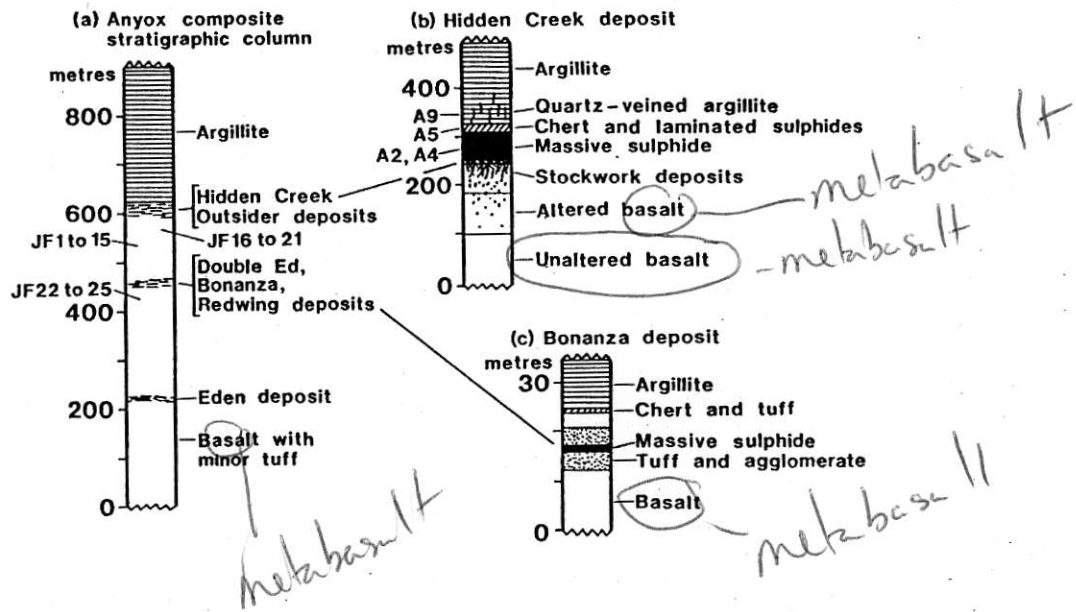
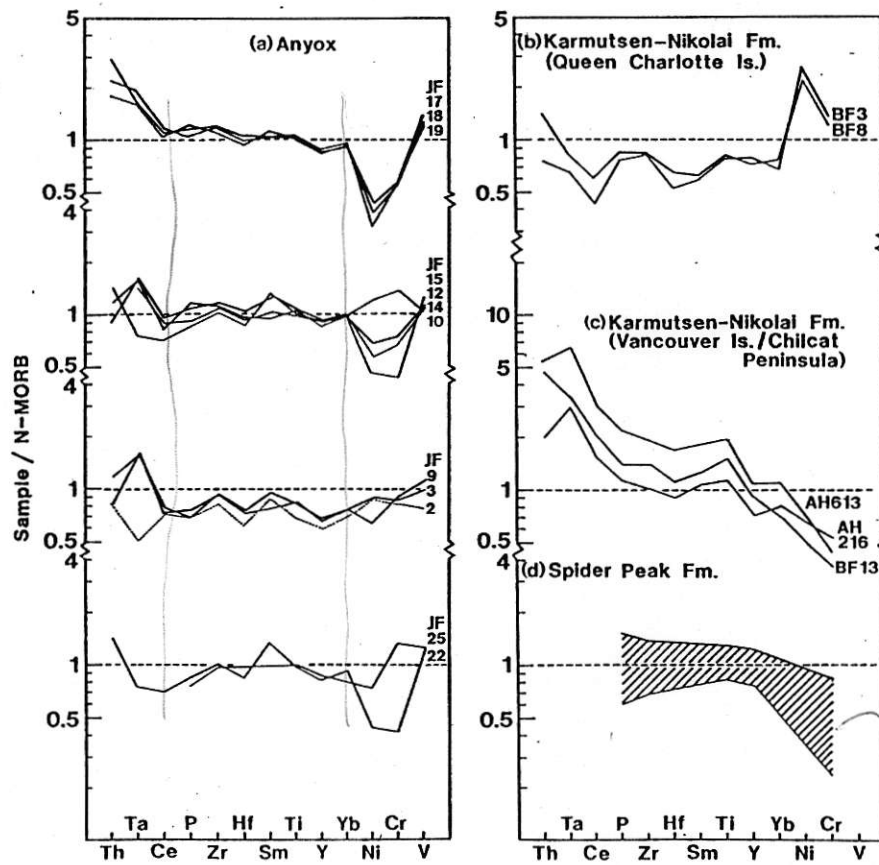
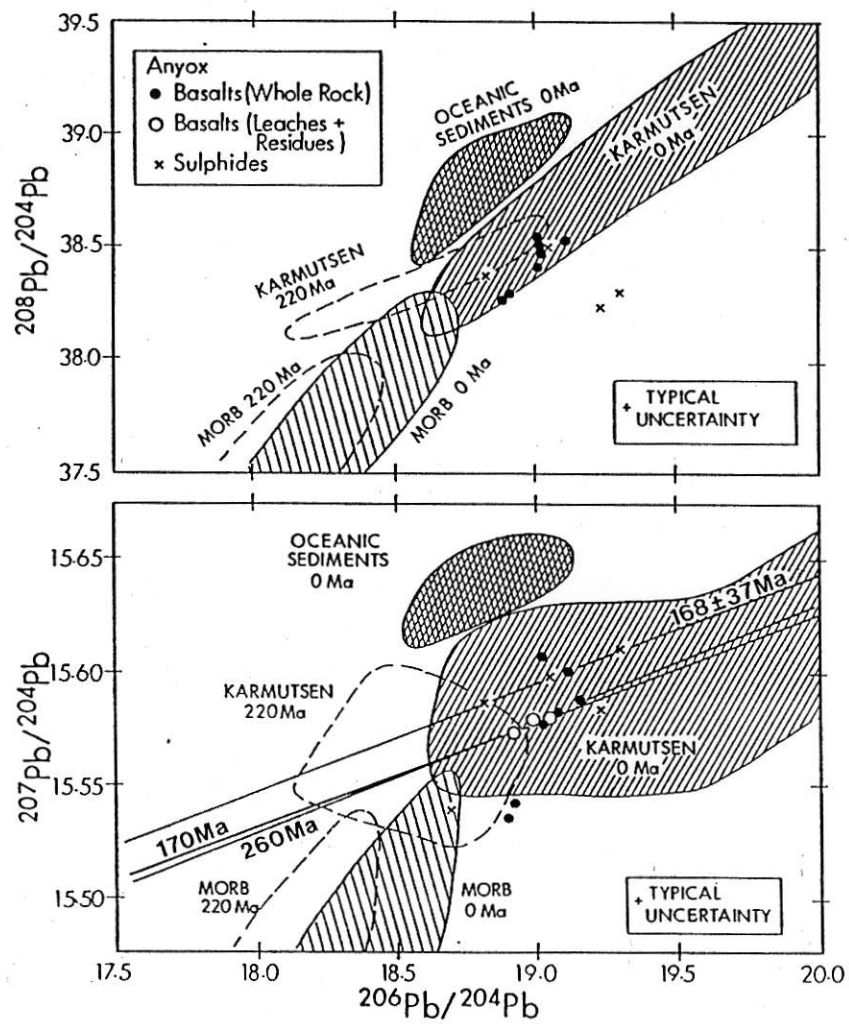


FIG. 3



not significant?

FIG. 4



other data?
Meth analyses

FIG. 5

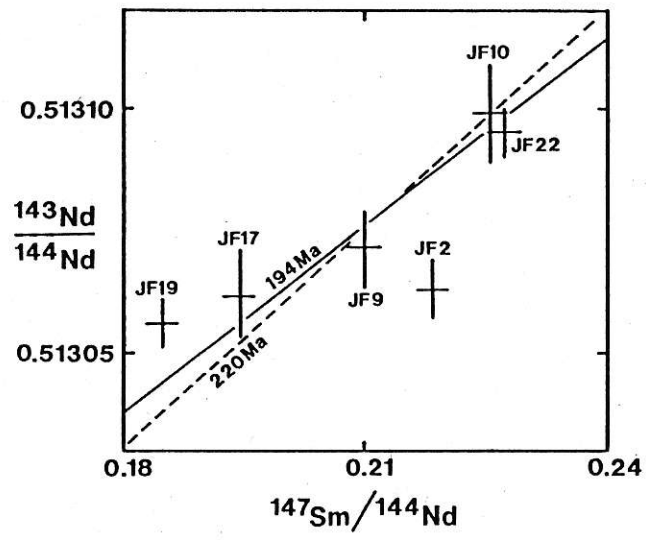


FIG. 6

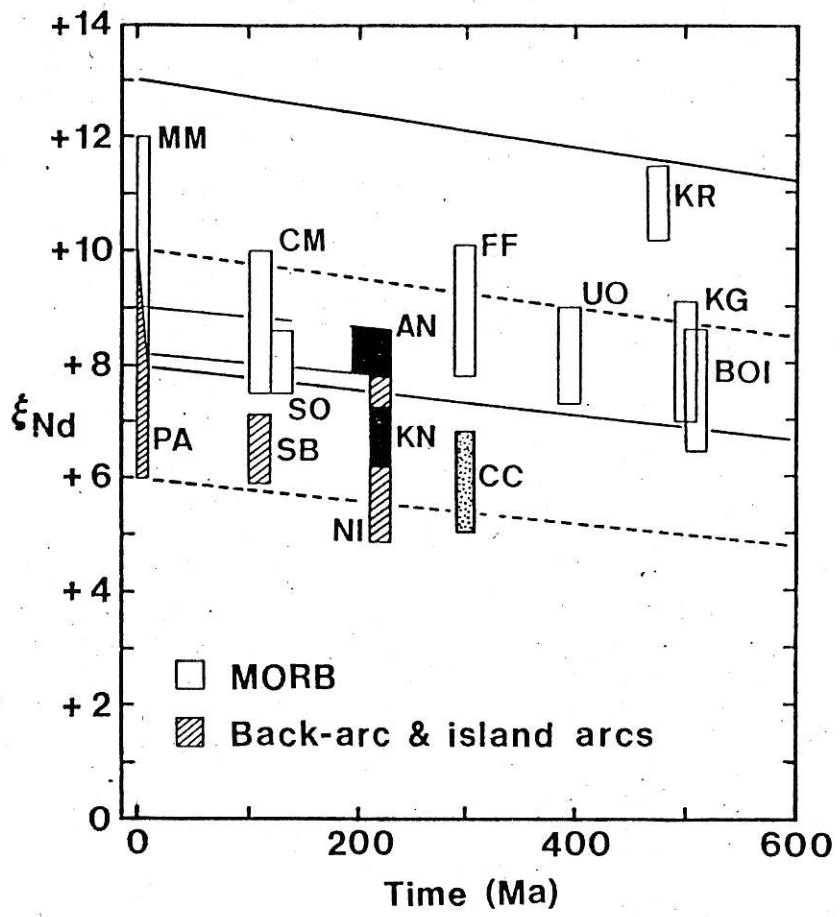
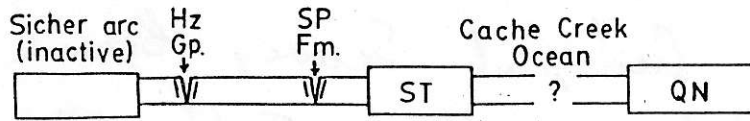
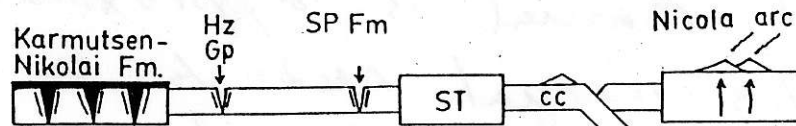


FIG. 7

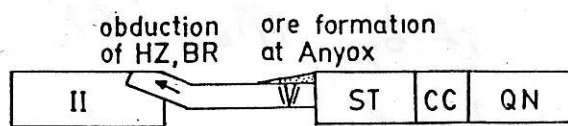
(a) Late Permian to Early Triassic



(b) Late Triassic



(c) Early to Late Jurassic



(d) Mid Cretaceous

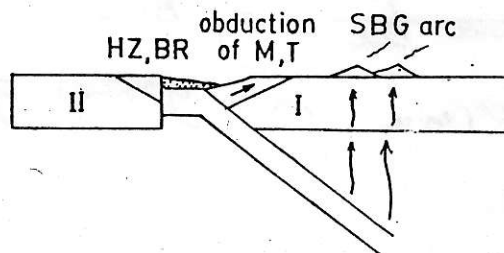


FIG. 8

INVITATION To QUOTE

The Geological Survey Branch requires an update to their Field Manual. The current manual is approximate - pages long. This manual needs to be updated and captured on diskette.

Need it by May 31.

Printed by Brim

preferably
Need to ~~have~~ be a B.Sc. geologist with field experience in ~~govt~~ mapping experience

\$12 on h
\$140 a day - 10 day project
\$1400

compatible with Word 5

